



# Topographical and morphological variability explicates the regional heterogeneity in glacier surface ice velocity across Karakoram-Himalaya

Naveen Tripathi<sup>\*</sup>, S.K. Singh, B.P. Rathore, S.R. Oza, I.M. Bahuguna

Space Applications Centre, ISRO, Ahmedabad, India

## ARTICLE INFO

### Keywords:

Glacier ice velocity  
Karakoram- Himalaya glaciers  
Feature tracking  
Regional variability  
Remote sensing  
Glacier dynamics

## ABSTRACT

Understanding the implications of variations in glacier surface ice velocity (SIV) has become an essential component of glacier research and monitoring. This study investigates the variability in SIV with respect to geography, morphology, and topography in Karakoram-Himalaya. SIVs are extracted for 1439 glaciers in the Karakoram-Himalaya region for the period 2016–2019 using Landsat-8 datasets and a feature tracking method. Glaciers are categorized based on their area, ice thickness, and ice volume in order to investigate the SIV variability with geographical, morphological, and topographical parameters. We highlight regional heterogeneities in glacier SIV across the Karakoram-Himalaya. We conclude that in addition to glacier morphology, the altitudinal heterogeneity of glaciers in the Karakoram-Himalaya best explains regional disparities in glacier SIV. For all glacier areas smaller than 20 km<sup>2</sup>, a significant negative correlation (less than −0.4) is observed between glacier minimum elevation and SIV. Heterogeneity in the role of elevation on SIV is also observed at the sub-basin scale, with a correlation of −0.47, −0.33, and −0.18 in the Hanza, Chenab, and Kosi sub-basins, respectively. An unsystematic variability of SIV for large glaciers (area > 20 km<sup>2</sup>), located mostly in the Karakoram and Western Himalayan regions, suggests that the elevation and sub-glacial hydrology may have a significant impact on their dynamics.

## 1. Introduction

Deriving surface ice velocity (SIV) of glaciers from optical or microwave images and understanding the implications of its variability have now been recognized as an essential element in glacier research. Recently, numerous regional to global-scale studies on the monitoring and variability of ice velocities have been reported (Dehecq et al., 2015; Maurer et al., 2019; Sam et al., 2018). This has been facilitated by the availability of a staggering amount of earth observations (EO) data and sophisticated data processing techniques or skills. A recent review of time series data of SIV for global glaciers indicates that Himalayan glaciers have slowed down since 2000 as a result of the volume decrease (Dehecq et al., 2019). Ice velocity is governed by a range of factors, including the ice thickness distribution from the glacier's terminus to its head, surface slope, mass balance, ice temperature, etc. (Benn and Evans, 2010; Cuffey and Paterson, 2010). Besides these factors, basal slip plays an important role in poly-thermal and temperate glaciers, as meltwater infiltrates and lubricates the glacier's base during the summer (Hubbard et al., 2000; Kamb and Echelmeyer, 1986; Singh et al., 2021). Precipitation and ablation patterns govern the distribution and intensity of glaciation throughout the Karakoram-Himalaya region (Kulkarni et al., 2010; Rathore et al., 2022) (Fig. 1a). Depending on the climatically sensitive zones and altitude, the wide vari-

<sup>\*</sup> Corresponding author. Space Applications Centre, ISRO, Jodhpur Tekra, Ahmedabad, 380015, India.

E-mail address: [naveent@sac.isro.gov.in](mailto:naveent@sac.isro.gov.in) (N. Tripathi).

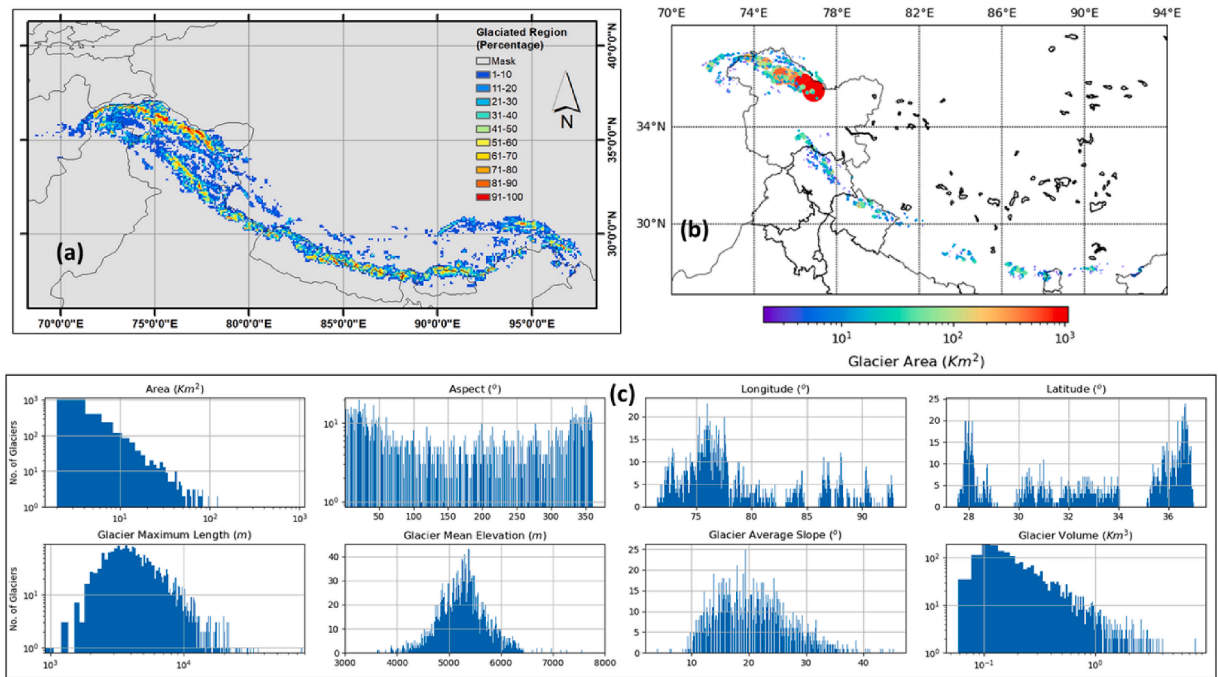


**Fig. 1.** (a) Percentage of glaciated area across Indus, Ganga, and Brahmaputra basins of Karakoram-Himalayas at  $0.1^\circ$  grid interval derived from SAC glacier inventory (Sharma et al., 2013). Most of the glaciated regions are covered for analysis. (b) Locations of 1439 glaciers covered in the study, having individual areas greater than  $2 \text{ km}^2$ . (c) Histogram distribution of various glacier parameters for 1439 glaciers covered in the study. Glacier volume is derived using ice thickness distribution from the new H-F model (Farinotti et al., 2019).

**Table 1**

Details of the data used in the study.

Data	Description			Spatial Resolution
<b>Landsat-8/Operational Land Imager (OLI) (Band-8/Panchromatic)</b>	<b>Path/Row</b>	<b>Pair-1</b>	<b>Pair-2</b>	15 m
	151/34	02 Oct 2017	22 Sep 2019	
	148/35	08 Sep 2016	29 Oct 2017	
	149/35	01 Aug 2017	24 Sep 2019	
	150/35	09 Sep 2017	12 Sep 2018	
	151/35	19 Sep 2018	22 Sep 2019	
	147/37	03 Oct 2016	20 Sep 2017	
	148/37	08 Sep 2016	29 Aug 2018	
	146/38	28 Oct 2016	31 Oct 2017	
	147/38	19 Oct 2016	20 Sep 2017	
	144/39	14 Oct 2016	23 Oct 2019	
	145/39	21 Oct 2016	24 Oct 2017	
	142/40	19 Oct 2017	09 Oct 2019	
	136/41	20 Oct 2015	22 Oct 2016	
	137/41	29 Oct 2016	17 Sep 2018	
	138/41	20 Oct 2016	26 Oct 2018	
	139/41	09 Oct 2015	27 Oct 2016	
	140/41	30 Sep 2015	20 Oct 2017	
<b>Randolph Glacier Inventory (RGI 6.0)</b>	Used for identifying glaciers and for glacier characteristics & topographic parameters			–
<b>Global Ice Thickness Dataset (Farinotti et al. 2019)</b>	Used for categorizing glaciers based on their ice thickness and volume			50 m

ation in snow accumulation and glacier ablation patterns affect glacier dynamics and mass balance in the region (Benn and Evans, 2010; Bahuguna et al., 2021; Rathore et al., 2018). SIV is also an important parameter for accessing the ice thickness or volume of glacier. Using the laminar flow method and Glen's flow equations, the glacier SIV and surface slope can be utilized to estimate glacier ice thickness (Gantayat et al., 2014). Recently, this approach has been implemented to estimate the volume of the worldwide glaciers (Millan et al., 2022). The earlier method of glacier volume estimation was using volume-area scaling (Bahr et al., 2015).

Image correlation techniques and D-InSAR techniques are the two major remote sensing techniques for retrieving SIV using optical and microwave datasets (Scambos et al., 1992; Bhattacharya and Mukherjee, 2017; Heid and Kääb, 2012; Tiwari et al., 2014). Image correlation techniques are widely recognized for extracting the SIV of glaciers in the Karakoram-Himalaya (Heid and Kääb, 2012; Copland et al., 2009; Huang and Li, 2011). It computes the period's displacement offset by cross-correlating two images acquired at

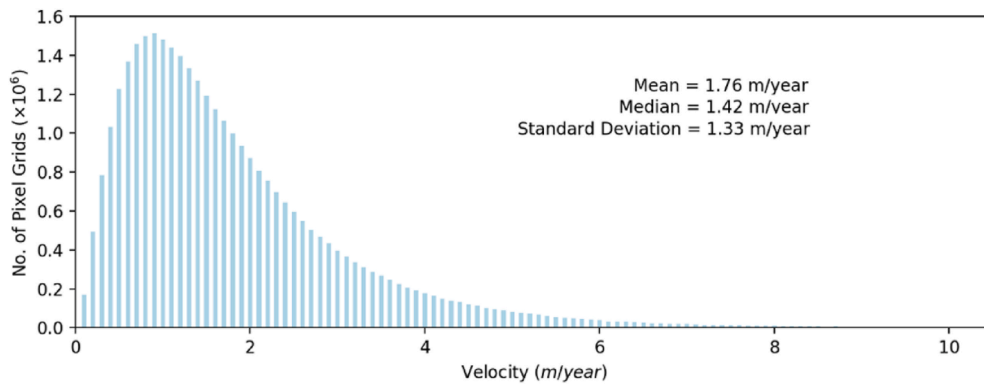


Fig. 2. Histogram distribution of velocity grids over the non-glaciated stable area. We have discarded the glaciers showing SIV less than 5 m/year.

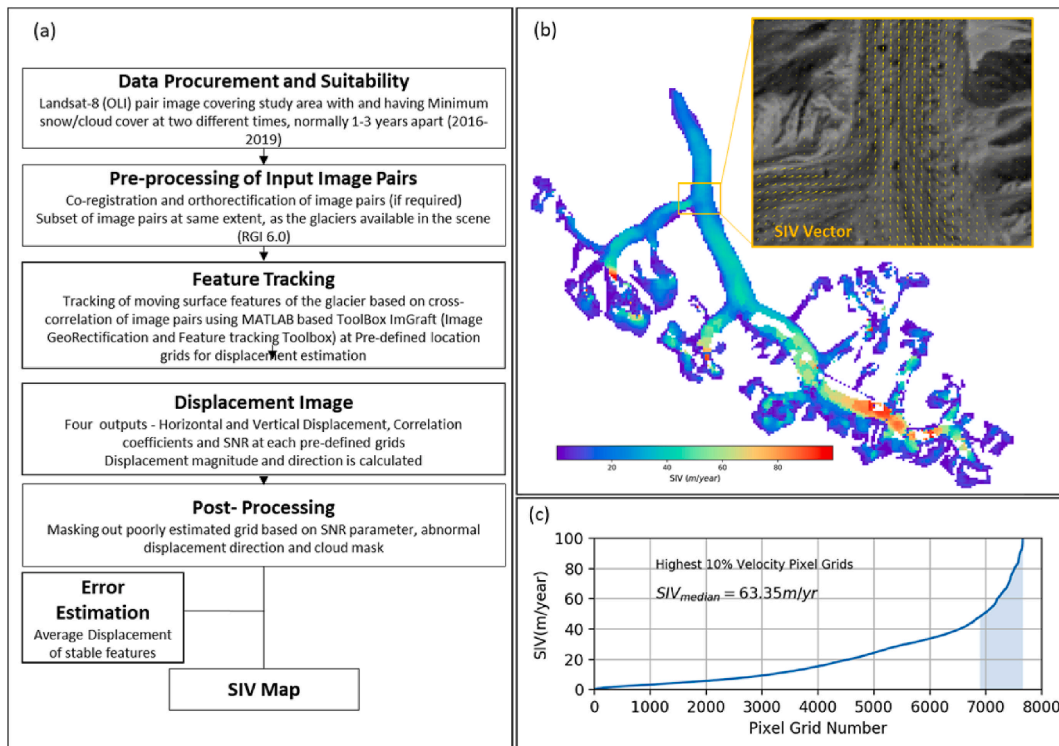


Fig. 3. (a) Flowchart of the methodology followed for SIV retrieval, (b) SIV layer for Gangotri glacier in Uttarakhand and the velocity vector at the conjunction with the tributary is shown at upper right, (c) The histogram of the velocity grids over the glacier and how maximum SIV calculated as median of 10 percent highest SIV grids.

different times. It involves the accurate tracking of glacier surface characteristics such as crevasses, humps, supra-glacial debris, and surface texture.

This study aims to investigate the regional variability in glacier SIV with respect to geography, morphology, and topography across 2400 km arcuate length of Karakoram-Himalaya. The objectives of the study involve (a) examining the regional variability in SIV across the Karakoram-Himalaya; (b) investigating the role of morphological and topographical parameters on glacier dynamics in Karakoram-Himalaya. SIVs of approximately 1400 glaciers are retrieved across the Karakoram-Himalaya region using the feature tracking approach. Landsat-8 datasets for the period 2016–2019 have been used, strictly considering data suitability favourable for feature tracking. The variability of glacier SIV is investigated with various geographical, morphological, and topographical parameters such as latitude, longitude, glacier sizes, elevations, surface slopes, hypsometry, etc. Glaciers are categorized based on existing ice thickness and volume estimates. Regional variability is examined for the three sub-basins in the Karakoram-Himalaya. Correlations of SIV with various glacier parameters are performed and the role of each of the parameters in controlling the SIV is investigated.

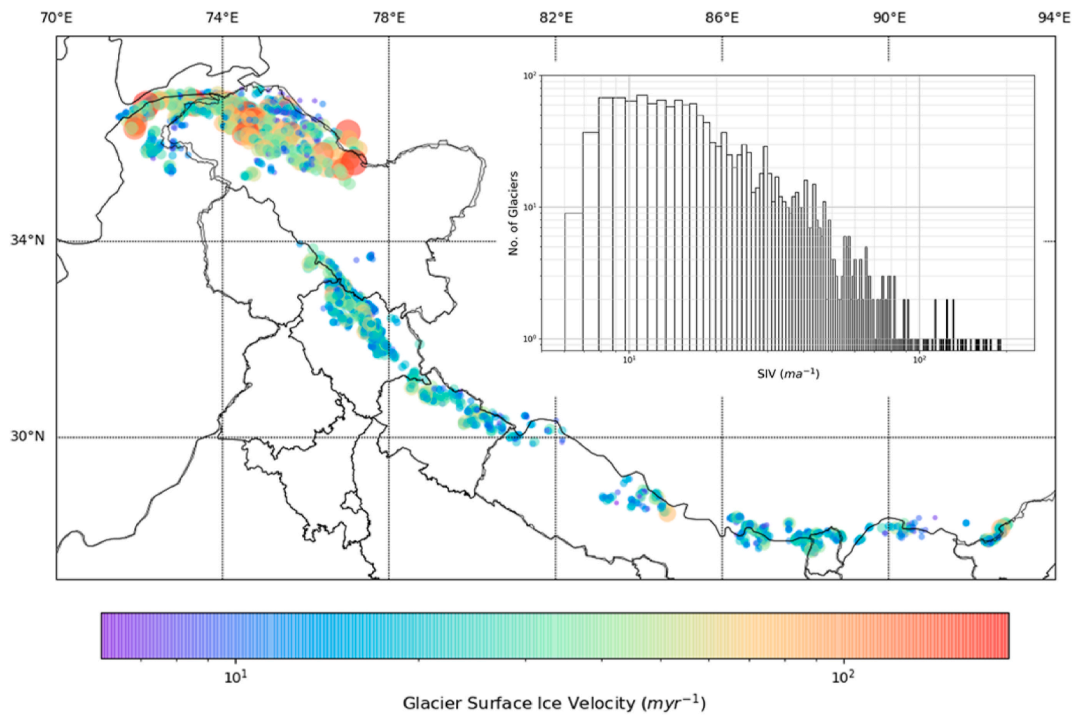


Fig. 4. Spatial distribution of SIV of Glaciers across Karakoram-Himalayas. Most of the higher glacier SIVs ( $>80$  m/year) is in Karakoram region.

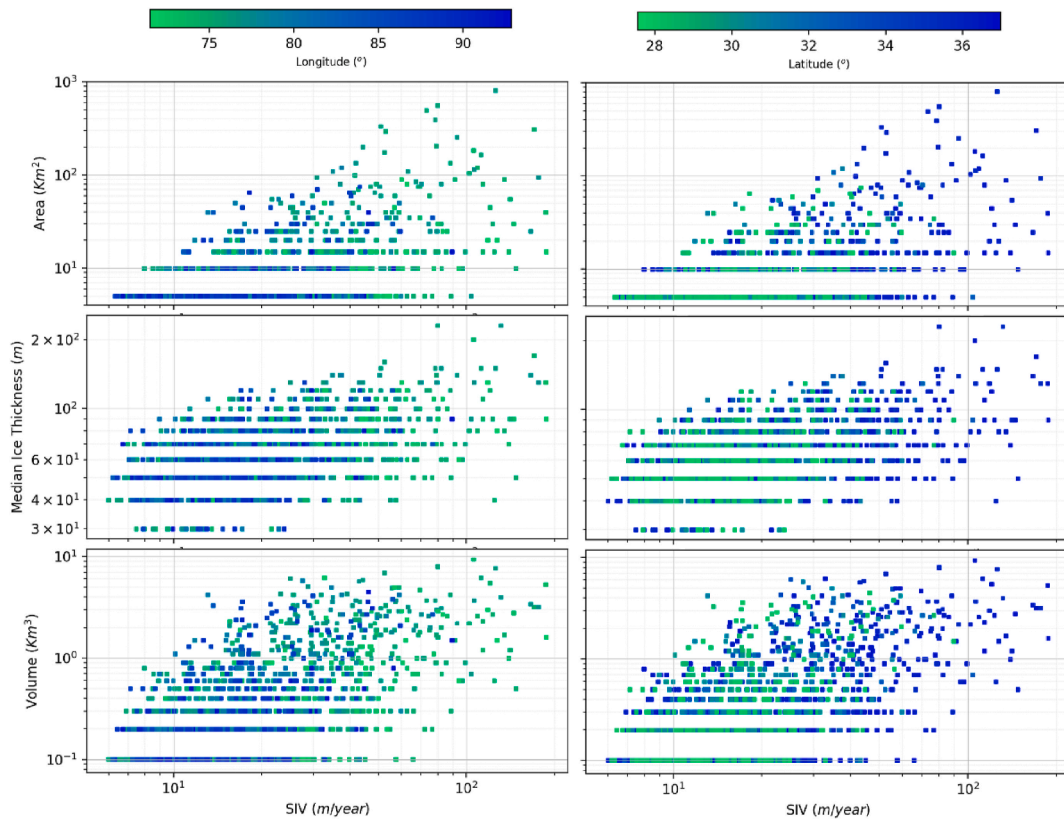


Fig. 5. Glacier SIV variability w.r.t latitude and longitude.



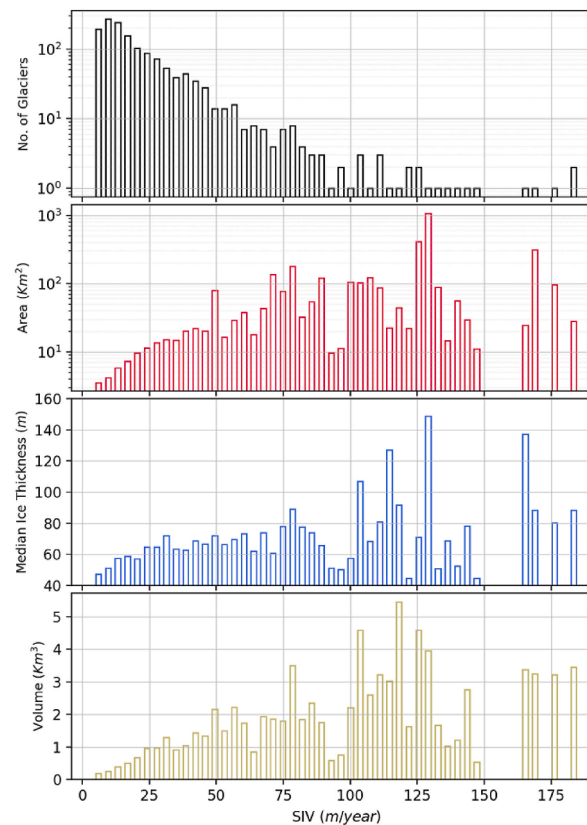


Fig. 6. Glacier SIV variability with glacier area, median ice thickness, and volume. The bar plot at top shows the number of glaciers exhibiting the particular SIV value.

## 2. Material and methods

Band-8 (panchromatic) from Operational Land Imager (OLI) of Landsat-8 is used for SIV retrieval using feature-tracking approach based on image cross-correlation. Based on the data's suitability for feature tracking, 17 pairs of datasets have been identified covering the Karakoram-Himalaya region between years 2017 and 2019 (Table 1). For accurate feature tracking, the glacier's surface features, such as crevasses, hummocks, and supra-glacial debris, must be exposed. The presence of snow or clouds may inhibit surface features; hence such datasets have been avoided. Post-monsoon and ablation months (August, September, and October) are favoured since they have the least amount of cloud cover and snowfall. For glaciers in Bhutan region, datasets during period 2015–2017 are used due to the non-availability of cloud-free datasets during the study period.

Randolph Glacier Inventory (RGI 6.0) has been used for glacier identification and delineation (RGI Consortium, 2017). Individual glacier characteristics have been taken from the attributes of the RGI 6.0, i.e. Area, Length, Elevations, Slope, etc. The global ice thickness dataset is used for deriving the median ice thickness and total ice volume of individual glaciers taken in the study (Farinotti et al., 2019).

This study examines the major portion of glaciated Karakoram-Himalaya region for which suitable datasets are available. It has been confirmed that the covered glaciers are uniformly distributed over the various glacier parameters, allowing for an accurate evaluation of the variability of SIV with respect to these parameters. Fig. 1b shows the locations of glaciers covered in the study, which are distributed along the stretch of Karakoram-Himalayas.

### 2.1. SIV retrieval

Open-source MATLAB-based toolbox- ImGRAFT (Image Georectification and Feature Tracking Toolbox) has been used for SIV retrieval. The tool can perform image georectification using Digital Elevation Model (DEM) and perform template matching between image pairs based on orientation image correlation (Messerli and Grinsted, 2015). Orientation image correlation involves the cross-correlation of angles of the intensity gradient at the pixels and it is found to be more effective in feature tracking over glaciers compared to the normalized cross-correlation technique. The template matching module of the ImGRAFT tool has been implemented with the Landsat-8 Operational Land Imager (OLI) panchromatic image pairs (Fig. 3a). Displacements are retrieved at a grid interval of four (60 m) using the defined template and search window size. An optimum template window size of 30 pixels and search window of 100 pixels are used. Displacement in the x and y directions, correlation coefficients, and Signal-to-Noise Ratio (SNR) at each defined grid are the outputs of the tool. The SNR is calculated as the ratio of the correlation coefficient of the best-matched template to the average correlation coefficients of all matched templates in the search area. It may be considered as a measure of the difference between

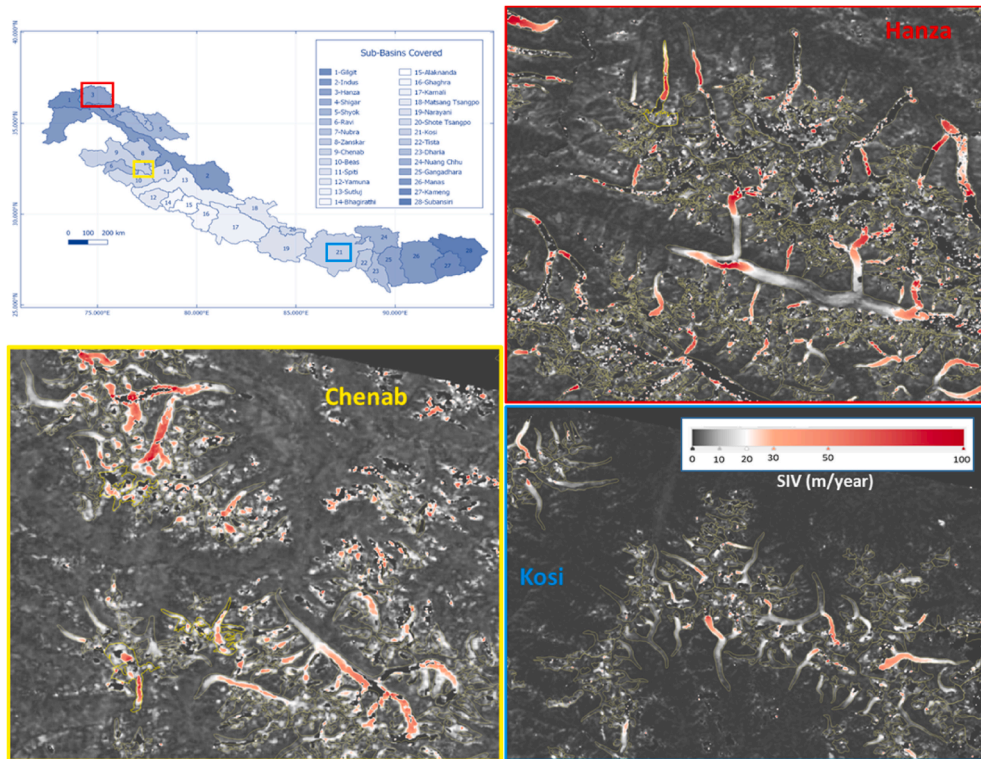


**Fig. 7.** The 28 sub-basins of Indus, Ganga, and Brahmaputra basins in Karakoram-Himalaya covered for the analysis and the SIV layer for three sub-basins that covers more than 100 glaciers: Hanza in West Karakoram, Chenab in Western Himalaya and Koshi in Central Himalaya. The rectangular box represents the particular region of the SIV layer and colors represents the sub-basin mentioned in the respective color. Red is the Hanza, Yellow is the Chenab and Blue is the Kosi. (For interpretation of the references to color in this figure legend, the reader is referred to the Web version of this article.)

the best-matching template and the other matched templates, and so reflects the correlation's quality. Therefore, greater SNR values suggest a good correlation grid. Each grid's SIV magnitude is determined using  $x$  and  $y$  displacements and the time between each pair.

## 2.2. Post-processing and error estimation

SIV vectors have been evaluated for all scenes, and it is observed that a filter based on SNR and aberrant SIV values ( $\text{SNR} > 6$  and  $\text{SIV} > 200$  m/year) effectively masked out the grids containing erroneous velocity vectors. Erroneous velocity vectors are typically the result of tracking false features with low correlation values, such as shadows, snow texture, or transient water channels; hence, they can be mostly masked out based on SNR value.

For each scene layer, the error in SIV magnitude has been approximated as the average velocity of non-glaciated stable features. Clouds and the incoherent surface characteristics, such as rivers, channels, snow, precipitation, can increase the velocity of stable features, which typically exhibit the lowest velocity. In general, these falsely correlated grids have low correlation and, hence, low SNR. The histogram distribution of velocity over non-glaciated stable grids with  $\text{SNR} > 6$  has been estimated for all scenes. The calculated mean, median, and standard deviation of velocity in metres per year are 1.76, 1.42, and 1.33, respectively (Fig. 2).

## 2.3. Glacier-wise SIV extraction

The Randolph Glacier Inventory (RGI 6.0) is used to identify glaciers, and SIV is extracted for each studied glacier. Only glaciers with a surface area higher than  $2 \text{ km}^2$  are considered in this study. For glacier-by-glacier SIV comparison, the mean, median, and maximum SIV values for each glacier polygon are determined. It is observed that glacier area correlates more strongly with maximum velocity than with average or median velocity. This could be because the calculated mean or median SIV values may depend on spatial distribution of the filtered SIV grids over a glacier. In order to avoid erroneous results while calculating the maximum SIV, the median of the 10 percent of the highest SIV grids over a glacier is estimated. (Fig. 3c). In addition, to make the analysis more accurate, the fraction of glacier area that is covered by the filtered SIV grids is calculated over each glacier. Glaciers with coverage area fraction less than 0.30 are discarded in the analysis. In addition, glaciers with a maximum calculated SIV of less than 5 m per year are excluded. Accordingly, the analysis includes a total of 1,439 glaciers.

## 2.4. Ice thickness and volume data

The median ice thickness and total ice volume of individual glaciers are estimated using a recently estimated global ice thickness dataset (Farinotti et al., 2019). As stated in Equation (1), the total ice volume is computed as the sum of the ice column volume at each

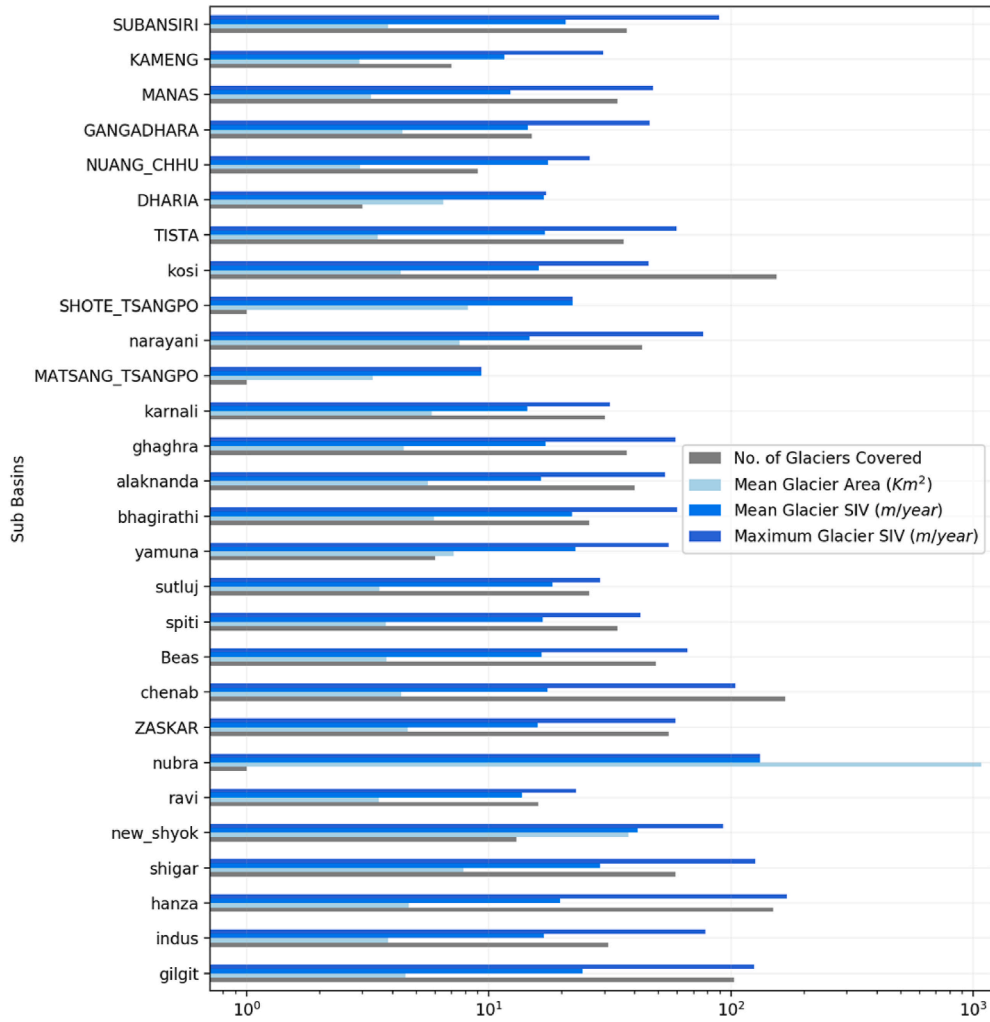


Fig. 8. The number of glaciers covered, mean glacier area, mean glacier SIV and maximum glacier SIV for each of the 28 sub-basins shown in Fig. 7.

pixel grid across a glacier. Simply put, the volume of the ice column at each pixel grid can be calculated by multiplying the ice thickness by the grid area.

$$Volume \text{ (in } Km^3) = \frac{1}{10^9} \sum_{Glacier} (Thickness \text{ (m)} \times 2500) \quad (1)$$

## 2.5. Glacier categorization based on area, ice thickness and volume

Glaciers are categorized based on three parameters that directly governs the driving stress: glacier area, median ice thickness, and total ice volume. Area, median ice thickness, and volume of glaciers are segmented at an interval of 5 km<sup>2</sup>, 10 m and 0.1 km<sup>3</sup>, respectively. Within each glacier category, the influence of morphological and topographical characteristics on glacier SIV is investigated.

## 2.6. Topographic parameters estimation

Glacier elevations from Randolp Glacier Inventory (RGI 6.0) are used in this study. Hypsometric Index (HI) is calculated (Equation (2)) for each glacier to categorized them into five categories based on HI: (1) Very top-heavy (HI < -1.5), (2) Top heavy (-1.5 < HI < -1.2), (3) equidimensional (-1.2 < HI < 1.2), (4) bottom-heavy (1.2 < HI < 1.5), and (5) very bottom-heavy (HI > 1.5) (Jiskoot et al., 2009).

The equation is shown below.

$$HI = \frac{(Maximum \text{ Elevation}) - (Mean \text{ Elevation})}{(Mean \text{ Elevation}) - (Minimum \text{ Elevation})} \quad (2)$$

if  $0 < HI < 1$ , then  $HI = \frac{-1}{HI}$

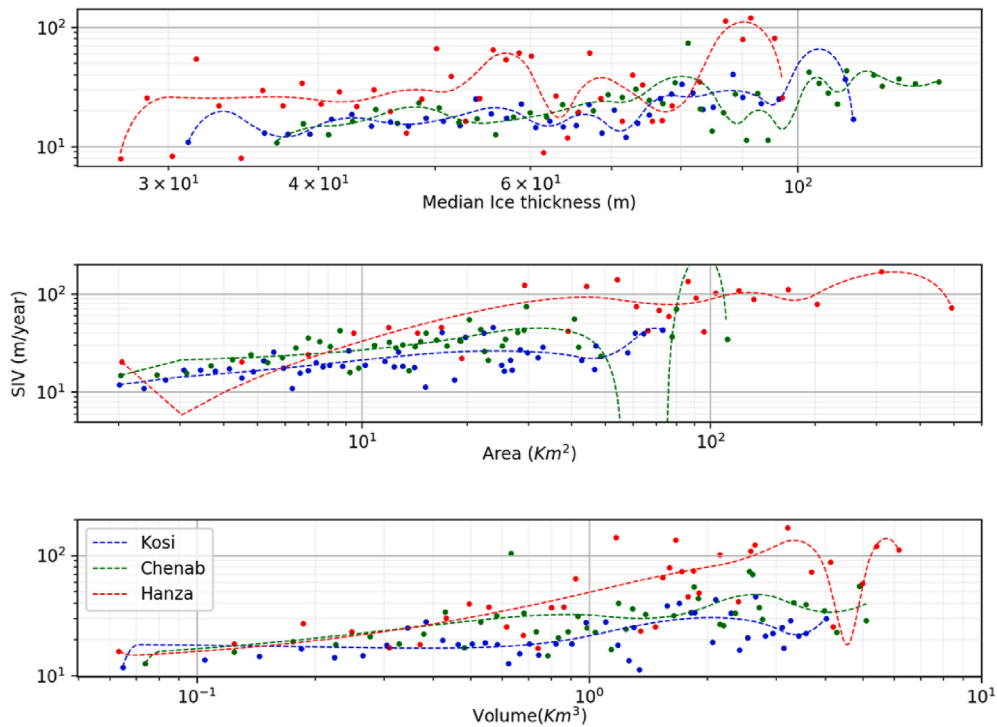


Fig. 9. Glacier SIV variability with median ice thickness, area, and volume for three sub-basins across Karakoram-Himalaya: Kosi, Chenab, and Hanza. The data points are fitted only for representation, using univariate spline from python scipy library.

### 3. Results

#### 3.1. SIV distribution and variability across Karakoram-Himalayas

Out of 1439 glaciers analyzed, 35 percent exhibit SIVs between 5 and 10 m per year, 45 percent have SIVs between 10 and 30 m per year, and 15 percent have SIVs between 30 and 60 m per year. 5 percent of glaciers have SIVs greater than 60 m per year, whereas 4 percent have SIVs between 60 and 100 m per year, and 1 percent have SIVs greater than 100 m per year (Fig. 4). Geographical distribution of SIV reveals that the majority of the highest glacier SIV is found in the Karakoram and Western Himalayas (Fig. 4). A greater degree of geographical or regional variation in SIV is observed when different glacier categories based on area, ice thickness, and volume are studied. Glaciers, with mean ice thicknesses between 30 and 90 m, have a distinct pattern of variation with latitude and longitude (Fig. 5). Glaciers in the Karakoram and Western Himalayas are found to have higher SIVs than those in the Central and Eastern Himalayas, particularly minor glaciers with area less than 20 km<sup>2</sup> (Fig. 5).

#### 3.2. Variation of SIV with respect to area, ice thickness, and volume

The primary control factor of glacier SIV is driving stress, and the area, ice thickness, and volume can be the indirect parameters to represent the driving stress. Hence, the variability of glacier's SIV with these parameters has been investigated at a binned interval of 4 m/year on SIV. A clear influence of area, ice thickness, and volume on SIV is observed, especially for glaciers with SIV in the range of 5–80 m/year (Fig. 6). Glacier SIV varies in a predictable way with glacier size up to 20 km<sup>2</sup>, but after that, the variabilities seem to be perplexing. Similar behavior is observed with total ice volume and median ice thickness. For glaciers with SIV larger than 80 m/year, which are mostly located in the Karakoram and Western Himalaya regions, no pattern of variation of SIV with area, ice thickness, or volume is seen, and their behaviour is atypical. This can be due to some other factors that dominantly control their dynamics.

#### 3.3. Regional variability at sub-basin scale

To observe how SIV varies across the sub-basins, 28 sub-basins (Fig. 7) have been selected that cover in our study region. For each sub-basin, the mean of glacier area & SIV and the maximum of glacier SIV are calculated (Fig. 8). Observation shows that the sub-basins in Karakoram and Western Himalayas contain glaciers having the highest SIVs. Further, we selected 3 sub-basins that cover more than 100 glaciers each: Hanza in the Karakoram; Chenab in Western Himalaya; Kosi in Central Himalaya; and analyzed the SIV variability with the area, ice thickness, and volume for each sub-basin (Fig. 9). Also the SIV for region in each sub-basin shown in Figure (8). Heterogeneity is observed in SIV variability with area, thickness, and volume among the three sub-basins. Glaciers in the Hanza sub-basin show the highest SIV (as high as ~100 m/year) for all glacier sizes. Kosi sub-basin exhibits the lowest SIV among the three sub-basins and Chenab shows intermediate behavior. A more evident dissimilarity is observed in the variation of glacier SIV with volume for the three sub-basins. The mean elevations of all the glaciated region for Hanza, Chenab, and Kosi sub-basins are estimated to be 5131m, 5030m, and 5779m, respectively, with the Kosi sub-basin having glaciers at a higher elevation.

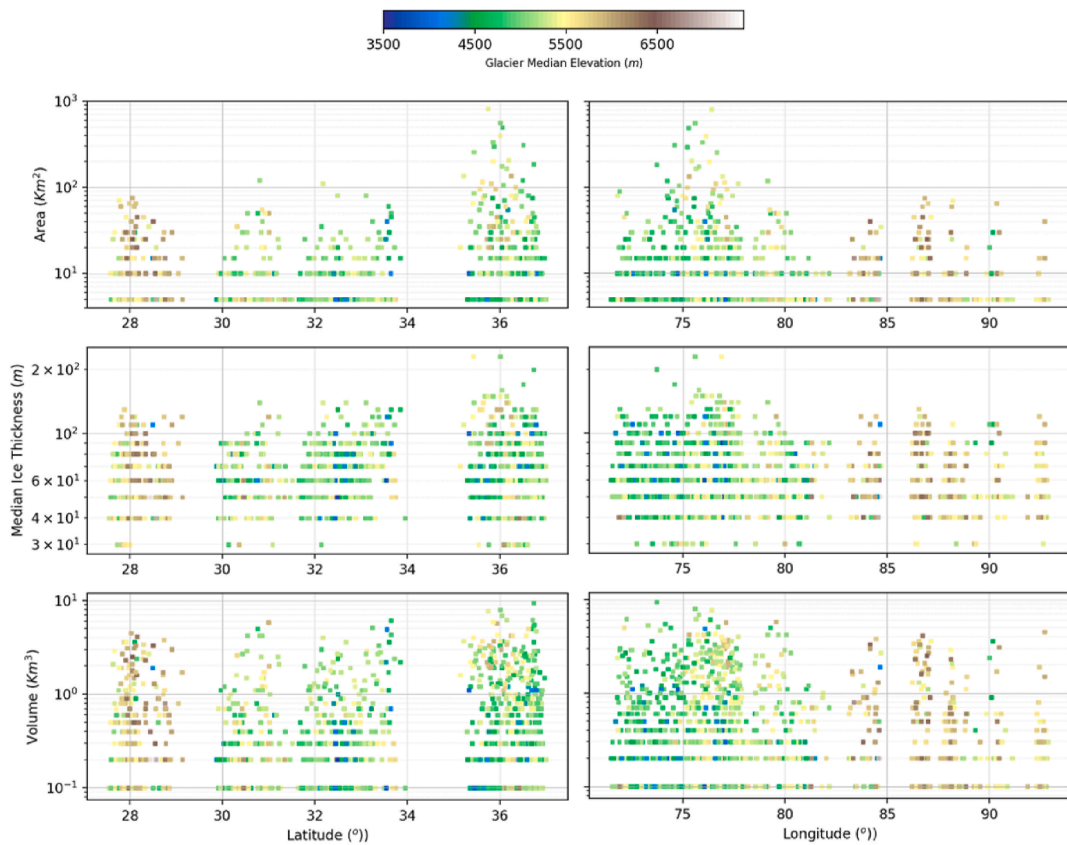


Fig. 10. Altitudinal variability of glaciers across Karakoram-Himalaya for different glacier categories based on area, ice thickness, and volume.

### 3.4. Altitudinal heterogeneity in glacier distribution across Karakoram-Himalaya

Glacier distribution in Karakoram Himalayas is examined concerning individual glacier elevation and a contrasting variability of glacier elevations is observed across the Karakoram-Himalayas for all the glacier categories. In the Karakoram and Western Himalaya, glaciers of comparable size are found to lie at lower elevations than in the Eastern or Central Himalayas. The difference in median elevations of similar size glaciers across Karakoram-Himalaya goes as high as  $\sim 2500\text{m}$  (Fig. 10). This much elevation variability would definitely affect the mass balance and glacier dynamics of the region.

### 3.5. Correlation of SIV with morphological and topographic parameters

Further to see the effect of morphological and topographic parameters on glacier SIV variability, the correlation is estimated between glacier SIV and the following morphological and topographical parameters: longitude, latitude, area, minimum elevation, maximum elevation, median elevation, slope, aspect, length, median ice thickness, volume, and hypsometric index. Nine glacier classes are considered based on glacier area varying from  $2\text{ km}^2$  to  $20\text{ km}^2$  at an equal interval of  $2\text{ km}^2$ . Larger glaciers have not been included as the number of glaciers for different glacier classes seems very less to observe any significant correlation. Further, for each glacier class, the Pearson coefficient of correlation between the glacier morphological or topographic parameters and glacier SIV is calculated (Fig. 11). A negative correlation is found with longitude with the Pearson coefficient of correlation varying from 0.1 (smaller glaciers) to 0.5 (medium-sized glaciers). A similar but positive correlation is observed with latitude with the coefficient of correlation going as high as 0.6. This clearly highlights the geographical variability in glacier SIV across the Karakoram-Himalaya. In addition, a positive correlation is observed with glacier average slope and the coefficient of correlation estimated to be around 0.2 for all the glacier sizes. However, no significant correlation is obtained with glacier aspect but a negative correlation with glacier hypsometric index is observed with coefficient of correlation estimated to be around  $-0.2$  for majority of the glacier classes. There was no significant correlation observed with glacier volume and median ice thickness; hence, the effect of these parameters on the variability of SIV within each glacier class can be eliminated. However, a positive correlation with glacier's maximum length and a significant negative correlation are obtained with both the glacier minimum and mean elevation for all glacier sizes.

Further analysis at sub-basin scale shows similar or more evident observations. Table 2 shows the correlation coefficients obtained for three sub-basins separately. Here, we have considered all the glaciers having an area in the range of  $2\text{--}20\text{ km}^2$  for correlation estimation. Although a positive correlation with area ( $> 0.41$ ) is obtained for all the sub-basins, there is distinguishability for the three sub-basins in correlation with the glacier elevation and slope. The correlation with glacier minimum elevation in the Hanza sub-basin



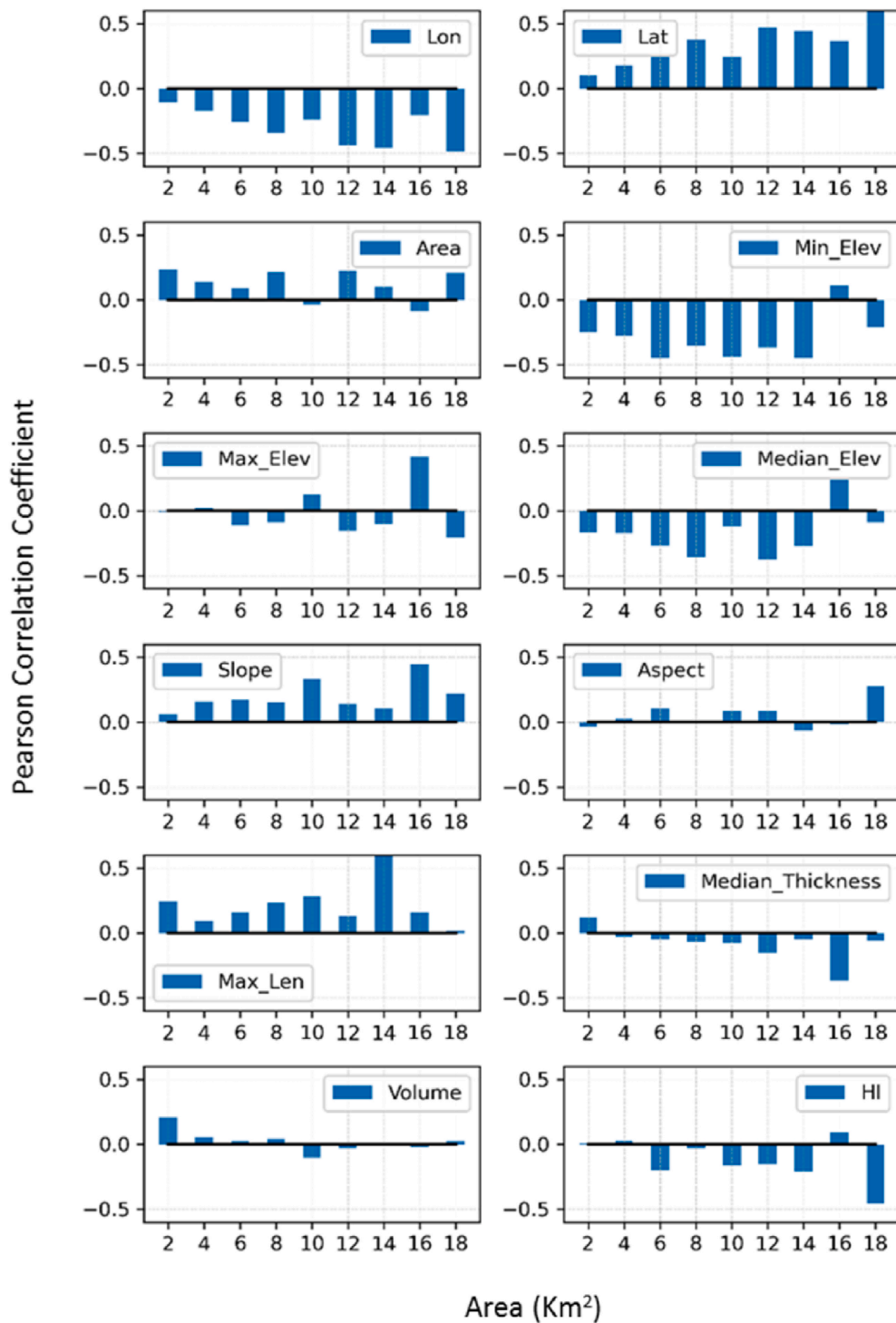


Fig. 11. Pearson correlation coefficients for different glacier sizes of correlation between SIV and various glacier and topographic parameters such as longitude, latitude, area, minimum elevation, maximum elevation, median elevation, slope, aspect, length, median ice thickness, volume and hypsometric index. X-axis represents the glacier area binned at an interval of 2  $\text{km}^2$ . All the glaciers in area range 2–20  $\text{km}^2$  are covered.

**Table 2**

Pearson correlation coefficients (p-value < 0.001) for correlation of the morphological and topographical glacier parameters with SIV for the three sub-basins, separately. Only glaciers in area range 2–20 km<sup>2</sup> are covered.

Glacier parameters	Pearson coefficients of correlation for individual glacier parameters and SIV for the three sub-basins		
	Hanza	Chenab	Kosi
Glacier Area	0.42	0.41	0.47
Maximum Length	0.46	0.32	0.42
Max Ice Thickness	0.42	0.47	0.31
Median Ice Thickness	0.22	0.33	0.24
Total Ice Volume	0.37	0.37	0.44
Minimum Elevation	−0.47	−0.33	−0.18
Median Elevation	−0.23	−0.07	0.06
Hypsometric Index	0.12	−0.19	−0.18
Average Surface Slope	0.17	0.17	−0.08
Glacier Aspect	−0.06	−0.03	−0.13
<b>No. of Glaciers covered</b>	<b>128</b>	<b>153</b>	<b>136</b>

(−0.47) is significantly higher than in the Chenab (−0.33) and Kosi (−0.18) sub-basins. Whereas, average surface slope shows a higher correlation of 0.17 for Hanza and Chenab compared to −0.08 in the Kosi sub-basin.

#### 4. Discussion

Basically, two components of glacier motion contribute to SIV, first one is the deformation velocity that majorly depends upon the ice thickness and surface slope (Cuffey and Paterson, 2010). The other one, basal sliding velocity, depends upon the resistive forces occurring opposite to the glacier motion. Both the components depend upon the ice temperature, ice mass and surface slope. The resistive forces are either applied through side valley walls or by the bedrock at the base of the glacier. The one through the side valley walls does not vary much seasonally when compared to the basal resistive force. This basal resistive force is often called basal shear stress and is majorly depends upon the glacier driving stress and sub-glacial water pressure. This basal resistive force varies seasonally as the sub-glacial water pressure varies throughout the year. This variation is due to changes in sub-glacial runoff and hydrology that increases the separation of ice mass and bedrock due to the formation of ice cavities and sub-glacial melt channels during summer. Hence the sliding velocity component varies seasonally with the amount of snow and glacier meltwater reaching the base of the glacier. Hence, any long-term (decadal) changes in glacier SIV may signify the changes in driving stress or the ice mass and the seasonal variations are explained by the changes in the basal sliding velocity or the sub-glacial hydrology. There is an observation that shows the influence of meltwater of tributary glaciers on the SIV of main glaciers (Singh et al., 2020). Many studies show the seasonal variations in SIV of Himalayan glaciers are highest in summer or ablation time and thus depends upon the melt-runoff (Satyabala 2016).

The regional variability of SIV for similar-sized glaciers can be explained as the precipitation, glaciation and ablation vary across Karakoram-Himalaya region (Bahuguna et al., 2021; Kulkarni et al., 2010; Rathore et al., 2022). Since we have analyzed the SIV variability separately in various glacier classes based on area and volume, the observed variability can mostly be due to the effect of parameters other than area, ice thickness or volume on SIV. We found glacier topographical parameters such surface slope, hypsometry and elevation together mostly explain the observed regional variability. A negative correlation with hypsometric index shows the very top heavy glacier (low HI) exhibits higher SIV and this is obvious as the glacier always try to be in equilibrium as per the mass conservation laws. However, for glaciers in Hanza, HI correlates positively with SIV (Table 2) and that may be because most of the glaciers belong to very bottom heavy to equidimensional category in the region. Similar role is played by glacier average slope and we observed a good and positive correlation (up to 0.4) with glacier SIV. At sub-basin level, a distinguishability can be seen in correlation of slope with SIV. Hanza and Chenab show a positive correlation with slope. Slope is very sensitive parameter in determining the glacier motion as both the components of glacier motion, deformation as well as basal velocity, are mostly influenced by the local surface slope.

Apart from the local topography affecting the glacier SIV, glacier's minimum or median elevation are found to be the best to explain this regional variability in SIV. The heterogeneous distribution of glaciers with respect to elevation across Karakoram-Himalaya region plays a key role in the regional variability of the glacier dynamics. Glacier minimum elevation and slope are found to explain the SIV variability more evidently in Hanza and Chenab sub-basin than in Kosi. Although the morphological parameters are found to influence SIV homogenously across Karakoram-Himalaya but the effect of topographical parameters, especially, glacier minimum elevation, slope or HI is significantly higher in Karakorum and Western Himalaya. Past study show that the mean glacier elevation and slope of the glacier tongue together explain most of the glacier-wide mass balance variability across Karakoram-Himalaya. (Brun et al., 2019). Elevation plays a significant role in the glaciation and ablation processes and it leads to the precipitation and ablation variability across the Karakoram-Himalaya. The variability in ablation patterns affects the glacio-hydrology of the region and hence the glacier dynamics. There are evidences that the structure of the sub-glacier drainage system of the glacier affects the basal sliding (Mair et al., 2002; Stevens et al., 2021). The growth of water filled cavities at the bed also controls the glacier speed-ups and this can also be influenced by the regional precipitations (Horgan et al., 2015). Though, this effect is only significant in summers but this will significantly contribute to the annual mean SIV of glaciers. Hence, the melt patterns over and below the glaciers affect the glacier dynamics (Stevens et al., 2021, Wyatt and Sharp, 2015).

The variation in the basal velocity factor in the Karakoram-Himalayas range is another probable conclusion that may be made from our analysis. Basal velocity factor is the ratio of basal sliding velocity to the surface ice velocity and it is generally taken as 0.25 in deriving the ice thickness estimates using glacier flow model based on shallow ice approximation method. The observed regional variability in SIV and glacier elevations, together, signifies the variability in the basal velocities of glaciers having similar ice thickness estimates. Considering the same basal velocity factor is one of the limitation in estimating ice thickness across the Karakoram-Himalaya region and it may lead to over or under estimation of ice thickness (Millan et al., 2022).

One of the limitations of our analysis is the consideration of a single SIV parameter for glacier-to-glacier comparisons. Based on ice thickness and surface slope, SIV varies along the glacier and is generally higher in the upper ablation region and decreases toward the terminus. Generally, glaciers are found to be the most dynamic in the upper ablation region as the ice thickness is the highest and the surface slope is not as gradual in the lower ablation region. Therefore, we assume that it is an appropriate location over a glacier for addressing SIV variability and glacier-specific comparisons. Another limitation can be that we have used glacier average slope for the variability analysis rather than local averaged surface slopes. The highest SIV values mostly lie in the upper ablation region of the glacier and thus we can expect relatively different local surface slopes at the location when compared with the glacier average slope. However, this variability can better be assessed by considering both the average surface slope and hypsometric index, together. In addition, correlation coefficients are calculated under the assumption that glacier parameters are independent, but, in reality, the vast majority of glacier characteristics are interdependent.

## 5. Conclusions

We have shown the regional variability in SIV across the stretch of Karakoram-Himalaya at the sub-basin scale and our analysis highlights the topographical and morphological variability of glaciers across Karakoram-Himalaya explicating the observed regional heterogeneities in SIV. Although the glacier ice thickness or area is found to be a major control factor for SIV (maximum correlation coefficients of 0.4) but the surface slope, hypsometry and, more notably, the elevation play a key role in controlling the dynamics, especially for glaciers below 20 km<sup>2</sup> area. Glacier minimum elevation shows a significant negative correlation ( $< -0.4$ ) with SIV for all the glacier sizes below 20 km<sup>2</sup> and at the sub-basin scale a correlation of  $-0.47$ ,  $-0.33$  and  $-0.18$  in Hanza, Chenab, and Kosi sub-basin, respectively. We highlight the heterogeneity in the extent of control of the topographical parameters across Karakoram-Himalaya, especially for the three sub-basins: Hanza in West Karakoram, Chenab in Western Himalaya, and Kosi in Central Himalaya. We conclude that in addition to glacier morphology, the altitudinal heterogeneity of glaciers in the Karakoram-Himalaya best explains regional disparities in glacier SIV. For larger glaciers, the unsystematic variability of SIV, especially in the Karakoram and Western Himalaya, signifies that the topography or sub-glacial hydrology may be considerably affecting the dynamics of the region. Our study adds some insights into the poorly understood dynamics of the Karakoram-Himalaya region and the variability in the extent of control of various morphological and topographical factors affecting the glacier dynamics.

## Author contributions

Conceptualization, N.T., I.M.B. and S.K.S; methodology, N.T. and S.K.S; resources, B.P.R. and S.R.O; data curation, N.T. and B.P.R; writing—original draft preparation, N.T. and S.K.S.; writing—review and editing, S.R.O and I.M.B; visualization, N.T.; supervision/project administration/funding acquisition, S.R.O. and I.M.B.

## Author statement

**Naveen Tripathi:** Conceptualization, methodology, data curation, writing—original draft preparation, visualization **S. K Singh:** Conceptualization, methodology, writing—original draft preparation **B. P Rathore:** resources, data curation **S. R Oza:** resources, project administration/funding acquisition, writing—review and editing **I.M Bahuguna:** Conceptualization, supervision/project administration/funding acquisition.

## Ethical statement

Hereby, I, Naveen Tripathi, consciously assure that all ethical practices have been followed in relation to the development, writing, and publication of the manuscript “*Topographical and Morphological Variability Explicates the Regional Heterogeneity in Glacier Surface Ice Velocity across Karakoram-Himalaya*”.

- 1) This material is the authors' own original work, which has not been previously published elsewhere.
- 2) The paper is not currently being considered for publication elsewhere.
- 3) The paper reflects the authors' own research and analysis in a truthful and complete manner.
- 4) The paper properly credits the meaningful contributions of co-authors and co-researchers.
- 5) The results are appropriately placed in the context of prior and existing research.
- 6) All sources used are properly disclosed (correct citation). Literally copying of text must be indicated as such by using quotation marks and giving proper reference.

## Declaration of competing interest

The authors declare that they have no known competing financial interests or personal relationships that could have appeared to influence the work reported in this paper.

## Data availability

Data will be made available on request.

## Acknowledgments

The work has been carried out under the project “Cryosphere Science and Applications Program” of Space Applications Centre, ISRO. We are grateful to Director, Space Applications Centre (SAC) for the administrative support in the project. We would like to show a courtesy to NASA Goddard Spaceflight Centre and U.S Geological Survey for acquisition and providing the Landsat imageries used in this study. We also thank all the researchers contributing to Randolph Glacier Inventory datasets used in our study. Also, we are grateful to Daniel Farinotti for openly providing the datasets of “a consensus estimate of ice thickness distribution of all glaciers on Earth”.

## References

- Bahr, D.B., Pfeffer, W.T., Kaser, G., 2015. A review of volume-area scaling of glaciers. *Rev. Geophys.* 53 (1), 95–140.
- Bahuguna, I., Rathore, B.P., Jasrotia, A.S., Randhawa, S.S., Yadav, S.K.S., Ali, S., Sharma, S., 2021. Recent glacier area changes in Himalaya–Karakoram and the impact of latitudinal variation. *Current Sci.* 121 (7), 929.
- Benn, D.I., Evans, D.J.A., 2010. *Glaciers and Glaciation*. Hodder Education, London, UK. 802.
- Bhattacharya, A., Mukherjee, K., 2017. Review on InSAR based displacement monitoring of Indian Himalayas: issues, challenges and possible advanced alternatives. *Geocarto Int.* 32 (3), 298–321.
- Brun, F., Wagnon, P., Berthier, E., Jomelli, V., Maharjan, S.B., Shrestha, F., Kraaijenbrink, P.D.A., 2019. Heterogeneous influence of glacier morphology on the mass balance variability in High Mountain Asia. *J. Geophys. Res.: Earth Surf.* 124 (6), 1331–1345.
- Copland, L., Pope, S., Bishop, M.P., Shroder, J.F., Clendon, P., Bush, A., et al., 2009. Glacier velocities across the central Karakoram. *Ann. Glaciol.* 50 (52), 41–49.
- Cuffey, K.M., Paterson, W.S.B., 2010. *The Physics of Glaciers*. Academic Press.
- Dehecq, A., Gourmelen, N., Trouvé, E., 2015. Deriving large-scale glacier velocities from a complete satellite archive: application to the Pamir–Karakoram–Himalaya. *Rem. Sens. Environ.* 162, 55–66.
- Dehecq, A., Gourmelen, N., Gardner, A.S., Brun, F., Goldberg, D., Nienow, P.W., et al., 2019. Twenty-first century glacier slowdown driven by mass loss in High Mountain Asia. *Nat. Geosci.* 12 (1), 22–27.
- Farinotti, D., Huss, M., Fürst, J.J., Landmann, J., Machguth, H., Maussion, F., Pandit, A., 2019. A consensus estimate for the ice thickness distribution of all glaciers on Earth. *Nat. Geosci.* 12 (3), 168–173.
- Gantayat, P., Kulkarni, A.V., Srinivasan, J., 2014. Estimation of ice thickness using surface velocities and slope: case study at Gangotri Glacier, India. *J. Glaciol.* 60 (220), 277–282.
- Heid, T., Käab, A., 2012. Evaluation of existing image matching methods for deriving glacier surface displacements globally from optical satellite imagery. *Rem. Sens. Environ.* 118, 339–355.
- Horgan, H.J., Anderson, B., Alley, R.B., Chamberlain, C.J., Dykes, R., Kehrl, L.M., Townend, J., 2015. Glacier velocity variability due to rain-induced sliding and cavity formation. *Earth Planet Sci. Lett.* 432, 273–282.
- Huang, L., Li, Z., 2011. Comparison of SAR and optical data in deriving glacier velocity with feature tracking. *Int. J. Rem. Sens.* 32 (10), 2681–2698.
- Hubbard, A., Willis, I., Sharp, M., Mair, D., Nienow, P., Hubbard, B., Blatter, H., 2000. Glacier mass-balance determination by remote sensing and high-resolution modelling. *Journal of Glaciology* 46 (154), 491–498.
- Jiskoot, H., Curran, C.J., Tessler, D.L., Shenton, L.R., 2009. Changes in Clemenceau Icefield and Chaba Group glaciers, Canada, related to hypsometry, tributary detachment, length–slope and area–aspect relations. *Ann. Glaciol.* 50 (53), 133–143.
- Kamb, B., Echelmeyer, K.A., 1986. Stress-gradient coupling in glacier flow: I. Longitudinal averaging of the influence of ice thickness and surface slope. *J. Glaciol.* 32 (111), 267–284.
- Kulkarni, A.V., Rathore, B.P., Singh, S.K., 2010. Distribution of seasonal snow cover in central and western Himalaya. *Ann. Glaciol.* 51 (54), 123–128.
- Mair, D., Nienow, P., Sharp, M., Wohlleben, T., Willis, I., 2002. Influence of subglacial drainage system evolution on glacier surface motion: Haut Glacier d’Arolla, Switzerland. *J. Geophys. Res. Solid Earth* 107 (B8). . EPM-8.
- Maurer, J.M., Schaefer, J.M., Rupper, S., Corley, A., 2019. Acceleration of ice loss across the Himalayas over the past 40 years. *Sci. Adv.* 5 (6), eaav7266.
- Messerli, A., Grinsted, A., 2015. Image georectification and feature tracking toolbox: ImGRAFT. *Geosci. Instrumentation, Methods and Data Syst.* 4 (1), 23.
- Millan, R., Mougnot, J., Rabatel, A., Morlighem, M., 2022. Ice velocity and thickness of the world’s glaciers. *Nat. Geosci.* 15 (2), 124–129.
- Rathore, B.P., Bahuguna, I.M., Singh, S.K., Brahmabhatt, R.M., Randhawa, S.S., Jani, P., et al., 2018. Trends of snow cover in western and West-Central Himalayas during 2004–2014. *Curr. Sci.* 114, 800–807. <https://doi.org/10.18520/cs/v114/i04/800-807>.
- Rathore, B.P., Bahuguna, I., Singh, S.K., Gupta, U.K., Randhawa, S.S., 2022. Monitoring snow cover in the Himalayan–Karakoram basins using AWiFS data: significant outcomes. *Current Sci.* 122 (11), 1305.
- RGI Consortium, 2017. *Randolph Glacier Inventory – A Dataset of Global Glacier Outlines: Version 6.0: Technical Report*, Global Land Ice Measurements from Space. Digital Media, Colorado, USA. <https://doi.org/10.7265/N5-RGI-60>.
- Sam, L., Bhardwaj, A., Kumar, R., Buchroithner, M.F., Martín-Torres, F.J., 2018. Heterogeneity in topographic control on velocities of Western Himalayan glaciers. *Sci. Rep.* 8 (1), 1–16.
- Satyabala, S.P., 2016. Spatiotemporal variations in surface velocity of the Gangotri glacier, Garhwal Himalaya, India: study using synthetic aperture radar data. *Rem. Sens. Environ.* 181, 151–161.
- Scambos, T.A., Dutkiewicz, M.J., Wilson, J.C., Bindshadler, R.A., 1992. Application of image cross-correlation to the measurement of glacier velocity using satellite image data. *Rem. Sens. Environ.* 42 (3), 177–186.
- Singh, G., Bandyopadhyay, D., Nela, B.R., Mohanty, S., Malik, R., Kulkarni, A.V., 2021. Anomalous glacier thinning due to climate feedback mechanism in the Himalaya and evidences in other mountain ranges. *Remote Sens. Appl. Soc. Environ.* 22, 100512.
- Singh, G., Nela, B.R., Bandyopadhyay, D., Mohanty, S., Kulkarni, A.V., 2020. Discovering anomalous dynamics and disintegrating behaviour in glaciers of Chandra-Bhaga sub-basins, part of Western Himalaya using D-InSAR. *Rem. Sens. Environ.* 246, 111885.
- Sharma, A.K., Singh, S.K., Kulkarni, A.V., 2013. Glacier inventory in Indus, Ganga and Brahmaputra basins of the Himalaya. *Natl. Acad. Sci. Lett.* 36 (5), 497–505.
- Stevens, L.A., Nettles, M., Davis, J.L., Creyts, T.T., Kingslake, J., Ahlstrøm, A.P., Larsen, T.B., 2021. Helheim Glacier diurnal velocity fluctuations driven by surface melt forcing. *J. Glaciol.* 1–13. <https://doi.org/10.1017/jog.2021.74>.
- Tiwari, R.K., Gupta, R.P., Arora, M.K., 2014. Estimation of surface ice velocity of Chhota-Shigri glacier using sub-pixel ASTER image correlation. *Curr. Sci.* 853–859.
- Wyatt, F.R., Sharp, M.J., 2015. Linking surface hydrology to flow regimes and patterns of velocity variability on Devon Ice Cap, Nunavut. *J. Glaciol.* 61 (226), 387–399.